Beam Physics Note
TRI-BN-23-12
April, 2023, updated Sept., 2024

Magnetic Measurement During the Cyclotron Main Magnet Ramp-up of April 2023

Thomas Planche, Paul Jung, Hui Wen Koay, Lige Zhang, Rick Baartman

TRIUMF

Abstract: This is a report on a series of measurements that took place in April 2023, during the ramp up of the TRIUMF 500 MeV cyclotron main magnet after shutdown. The purpose of these measurements was to establish a new procedure to ramp up the power supply to ensure a better reproducibility of the magnetic field. The purpose of this note is to present a summary of the experimental data that we have collected, and to discuss the resulting ramping procedure that was put to use for the rest of the operating year.

1 Introduction

A concern that has existed since first extracted beam 49 years ago, is the long startup times for the TRIUMF 500 MeV cyclotron. Often much tuning of trim coils is required, causing startup times of hours or even days. (One of the helpful techniques has been to pass the massive steel crane over the vault.) The lack of reproducibility is related to the magnet's large size and long time constants. Depending upon how the magnet shut down, whether planned or by a power failure of some kind, at the next ramp-up, the magnet as a whole does not reproduce its previous field to the level of precision required by the beam. This level of precision is a fraction of a gauss out of a peak field of 5600 gauss. It is conjectured that not all parts of the steel are at the same point in the hysteresis curve, when the coil is re-energized.

In 2016, the original power supply was replaced by one whose design was based upon those used in the CERN LHC.[1, 2]. Since this power supply replacement there has been a marked increase in difficulty in tuning the cyclotron, especially during recovery from an unexpected power trip.

For this reason, we began experimenting with new ramping procedures. For a small magnet, one can demagnetize first, using a bipolar power supply and running through successively smaller hysteresis loops, and then ramping up to required field. This technique is known to give good reproducibility. For the 18,000 Amp main magnet power supply, this is not practical. Instead, we try the new technique that had been developed for smaller unipolar cases[3]. This technique ramps the current cyclically about the desired setpoint to reach a reproducible field that is independent of its history. This note summarizes application and optimization of this technique to the main magnet.

1.1 Time Scales

Before proceeding to the experimental data, let's first develop a sense of scale of the magnet by looking at the typical magnet parameters, deriving its time scales and the field stability requirements. The new main magnet power supply is capable of outputting 20 kA at 80 V (1.6 MW). Originally, the power supply itself was current-stabilized, but this resulted in a stability of ±10 ppm. In the early 80s, a feedback loop was implemented based upon integrating the current induced in the outermost trim coil (TC54), supplemented with an NMR probe[4].

The magnet itself has resistance $R = 0.0039\,\Omega$ and inductance $L = 0.120\,\mathrm{H}$ for a time constant of $\tau = L/R = 31\,\mathrm{s}$. This is the scale of time for field fluctuations.

The stability requirements can be derived from the number of turns the particles make in the cyclotron currently 1700 (at the lowish rf dee voltage of 80 kV). Multiplied by the harmonic number $h = 5$, it is 8500 periods. Alternatively, knowing that the time of flight is $\sim 370\,\mu\mathrm{s}$, multiply by the rf frequency 23 MHz to get 8500, or 3 million degrees of RF. Thus to make the beam phase stable to a degree, need magnetic field stability of 1/3 ppm (part per million). Functionally, however, a stability of 10° is sufficient, or 3 ppm in the magnetic field.

From the time constant we can now derive how much time it takes for the field to reach this precision.

$$\exp[-t/\tau] < 3 \times 10^{-6}, \text{ or } t > 400\,\mathrm{s} \tag{1}$$

However, because of the huge mass of the cyclotron magnet, the time needed to reach thermal steady state is far longer than these 6 minutes. The magnet mass is 4×10^6 kg. It takes 420 J of energy to heat one kg of steel by 1K. Or 17 GJ to raise the cyclotron mass by 10K. For the typical current of 18 kA, or 1.3 MW power, it thus takes ~ 4 hours for the cyclotron magnet to reach a stable temperature.

Lastly, as discussed below (section 6), there is the time of propagation of magnetization. This is an effect of eddy currents, and is found to be about 20 minutes.

2 Experimental setup

Three Hall probes are temporarily installed on top on the cyclotron vacuum chamber as show in Fig. 1. Two of these probes (the "X" and "Y" channels, referred to as probe #1 and #2 hereunder) are inserted into the small space between the magnet pole and the vacuum chamber. The last one is attached to one of the vacuum chamber tie rods. If you are not familiar with the configuration, here is a good place to start [5]. The probes are

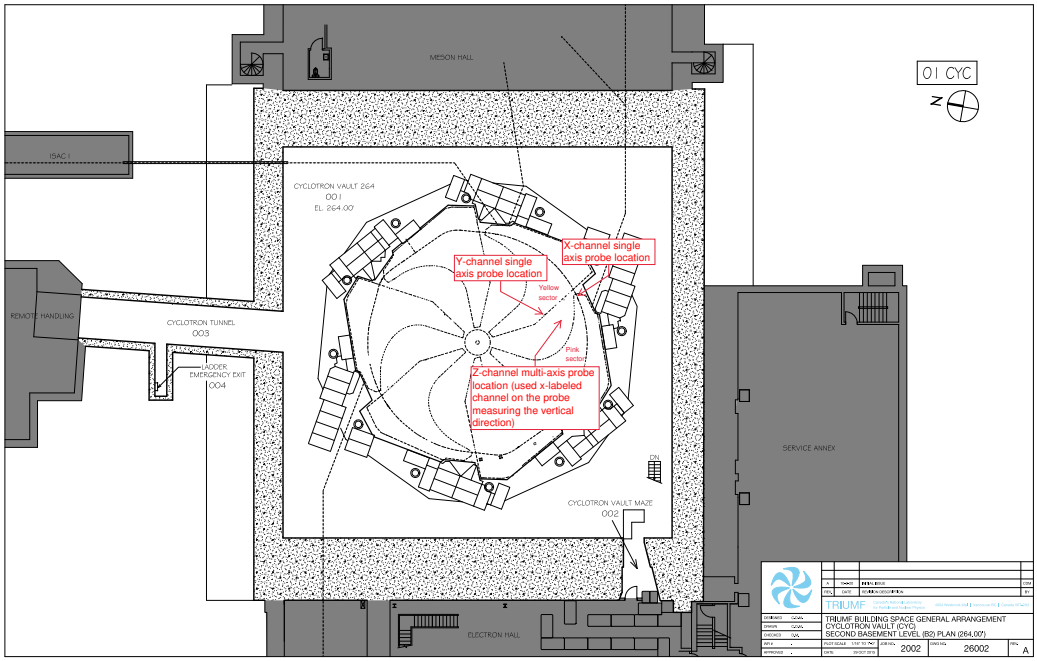

Figure 1: Location of the 3 Hall probes installed right on the top of the cyclotron vacuum chamber.

connected to a LakeShore 460 Gauss meter. The Gauss meter is read through a serial port connection (with the connector borrowed from Controls), connected to a laptop computer that was left in the accelerator vault. The computer is connected to the network using a long Ethernet cable (as there is no Wi-Fi in the vault). A simple `Python` script is left to run on the laptop which collects the probe data 4 times per second. The data from the main magnet power supply is read simultaneously using `jaya`, using a different script on our personal computers. All of the details on how we collected the data are available here: gitlab.triumf.ca/pjung/hall_probes.

3 Ramp up

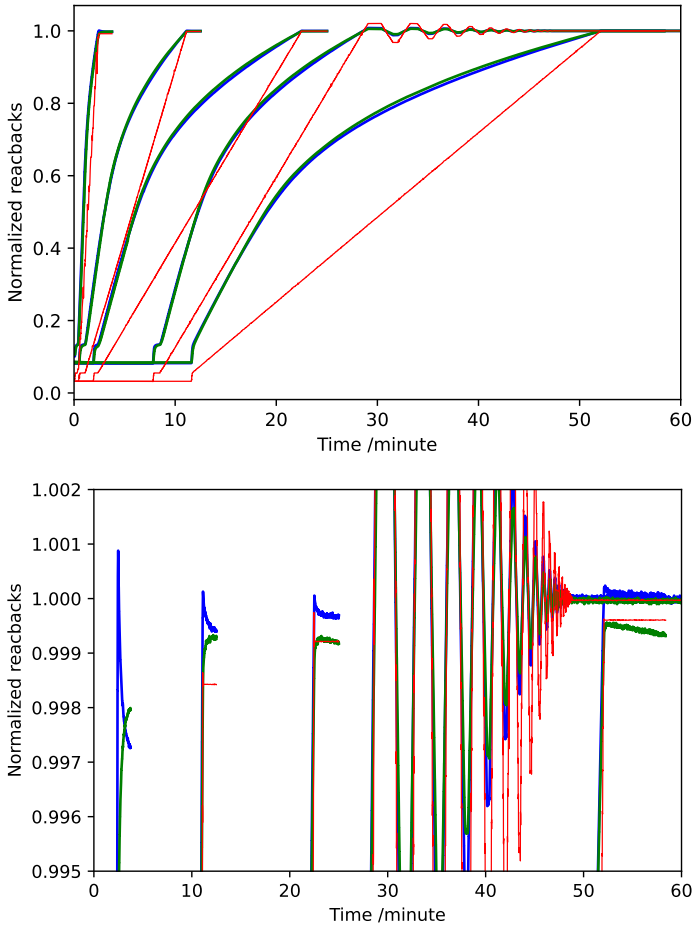

Figure 2: Different ramp up. The start time of each series of traces has been shifted so as to make them all fit nicely onto one plot. You can see in this order: a 2-min linear ramp, 10-min linear ramp, 20-min linear ramp, 20min+20min fancy ramp, and a 40-min linear ramp. The blue trace is from probe #1 divided by 5.4645 kG; the green trace if from probe #2 divided 5.8292 kG; the red trace is the magnet power supply read back, divided by 18130 A. The plot at the bottom is a zoomed-in version around the top of the ramps.

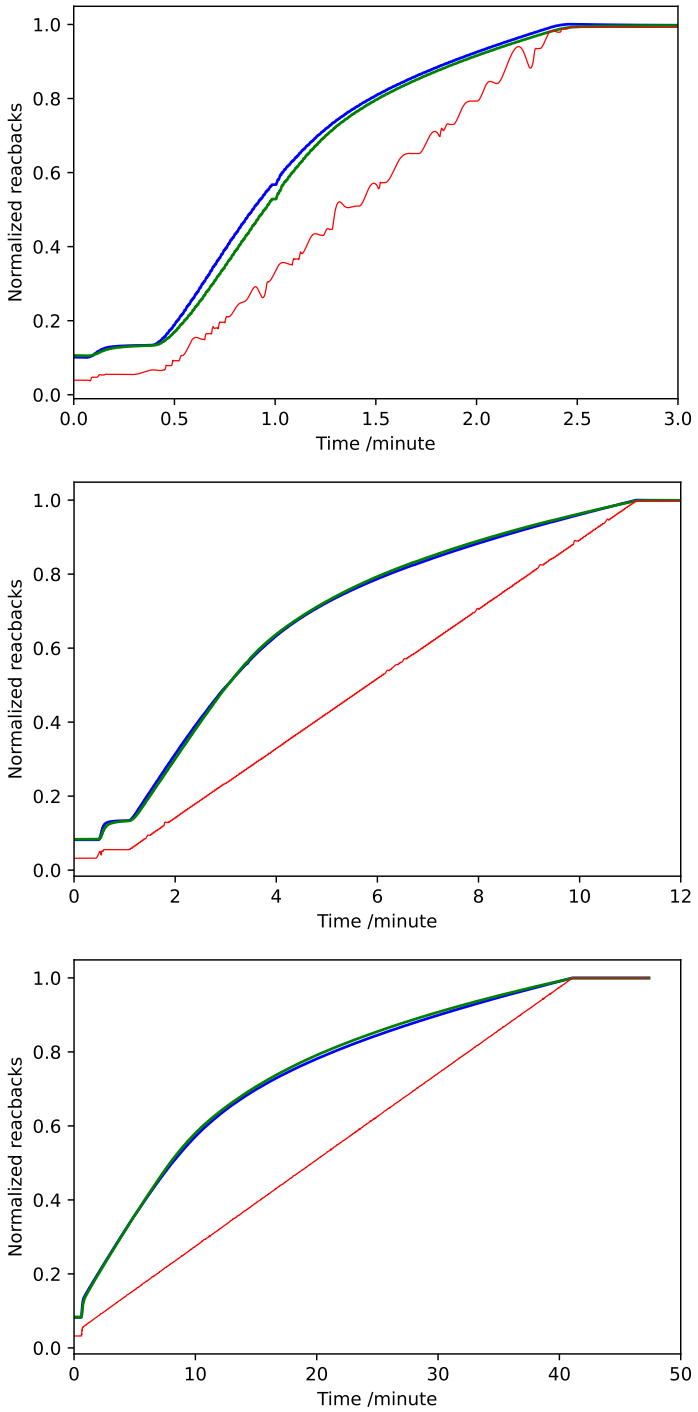

Figure 3: Same as the previous couple of plots, but only showing three distinct ramps: the 2-min, 10-min and 40-min linear ones.

4 B(I) curves

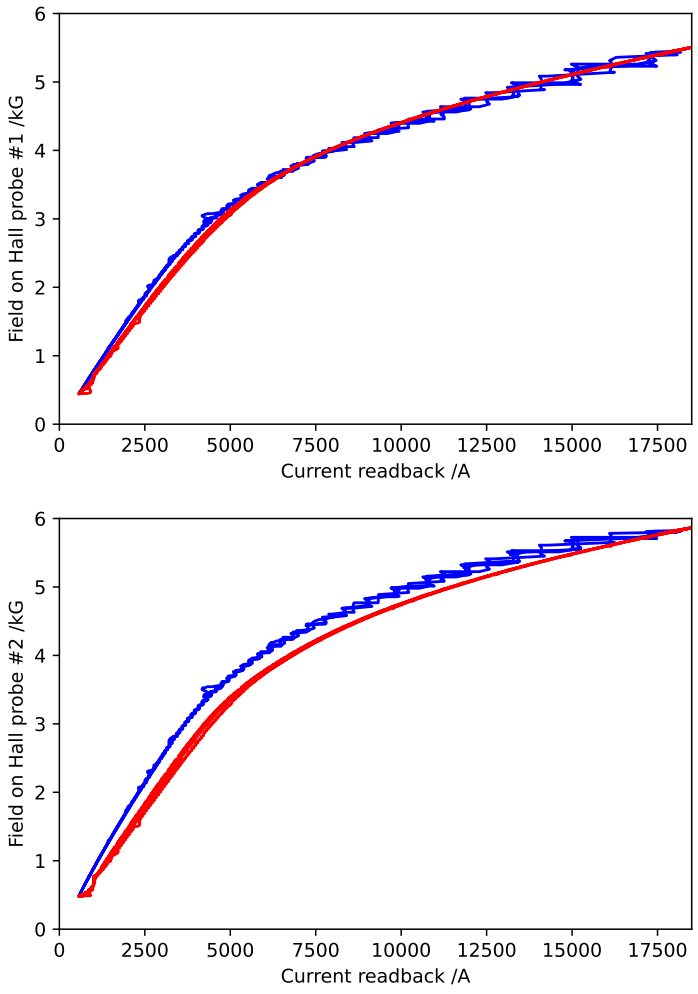

Figure 4: B(I) curves measured by probe #1 (top) and #2 (bottom) during the 10-min, 20-min, 40-min and fancy-set ramp up (red curves). The measurements taken during the corresponding ramp down are shown in blue. Data taken during the 2-min ramp up are shown in a separate plot as it is significantly more "noisy".

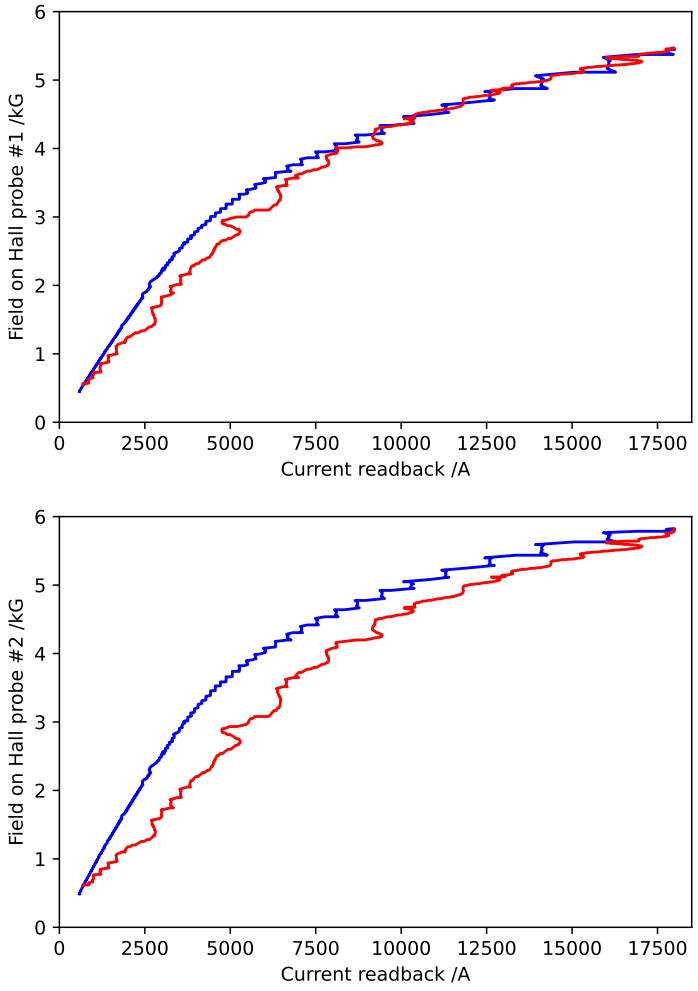

Figure 5: B(I) curves measured by probe #1 (top) and #2 (bottom) during the 2-min(red curves). The measurements taken during the corresponding ramp down are shown in blue.

5 Field Stability

5.1 "Bunny Test"

Before the test, the main magnet is ramped up via two different ramp-up procedures: fancy ramp-up and conventional ramp-up. Then, it is allowed to stabilize for $\sim$ 5 mins. During the "bunny test", several steps of $\pm$40 A and $\pm$80 A of coil current were applied in both directions for multiple times. The average magnetic field was determined using the NMR probe each time when the coil current is placed back to the set point. The outcome from the bunny test for the fancy ramp-up is compared to the one from the conventional ramp-up and the results are shown in Fig. 6.

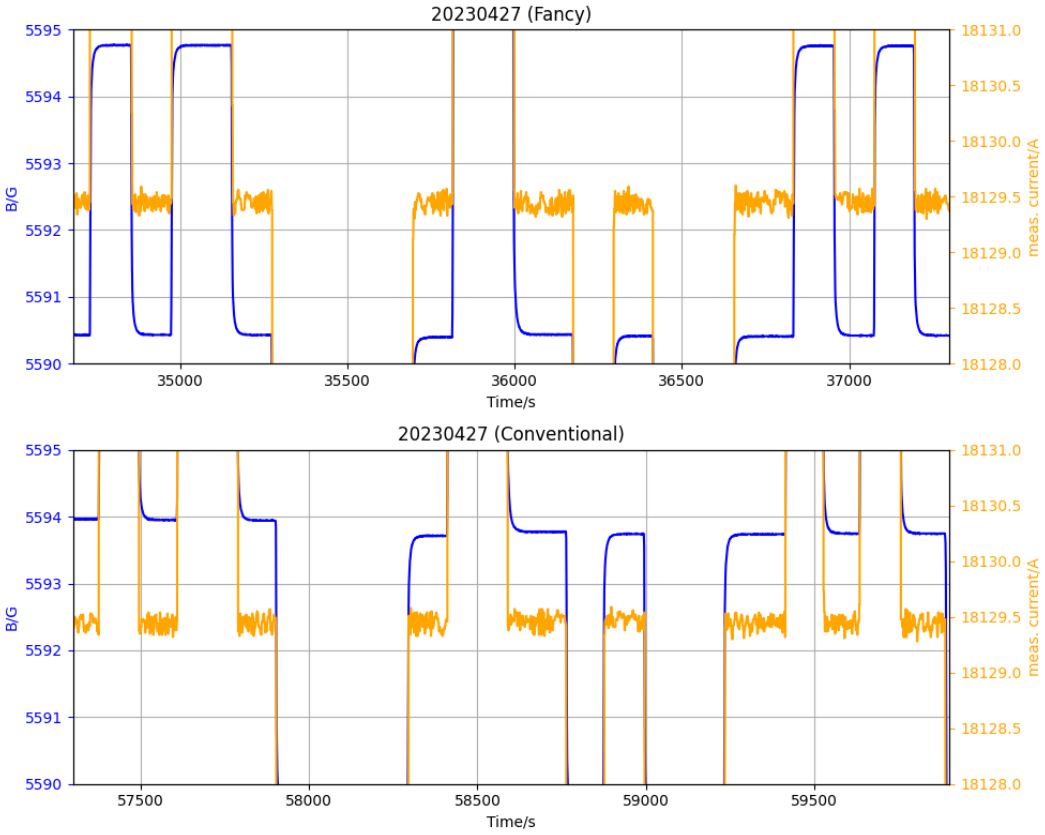

Figure 6: Results of the bunny test comparing the fancy ramp-up (top) and the conventional ramp-up (bottom). The maximum change of B field are 40 mG (fancy) and 250 mG (conventional) respectively, while the drift before and after the test are 20 mG (fancy) and 210 mG (conventional) respectively. Despite both of these tests were conducted on the same day (2023-04-27) at the same measured coil current of 18129.5 A (orange), the average magnetic field differs by about 3.5 G.

The magnetic field of the fancy ramp-up procedure shows almost an order of magnitude

improvement of the field reproducibility as compared to the conventional method. The maximum change of magnetic field after the fancy ramp-up is 210 mG better than the conventional set. The drift of the magnetic field before and after the bunny test is 190 mG less than conventional set. Therefore, we can conclude that the fancy ramp-up produces a more stable and reproducible field than the conventional way.

5.2 Crane Sweep

Similarly, the effect of a crane sweep procedure was investigated using the NMR probe. The results comparing the field from both ramp-up procedures are shown in Fig. 7 The largest bump created by crane-sweep is about 0.5 G. This is consistent with the observed value from similar test performed last year using the conventional ramp-up. However, the difference of magnetic field before and after the crane-sweep is slightly larger for the fancy ramp-up.

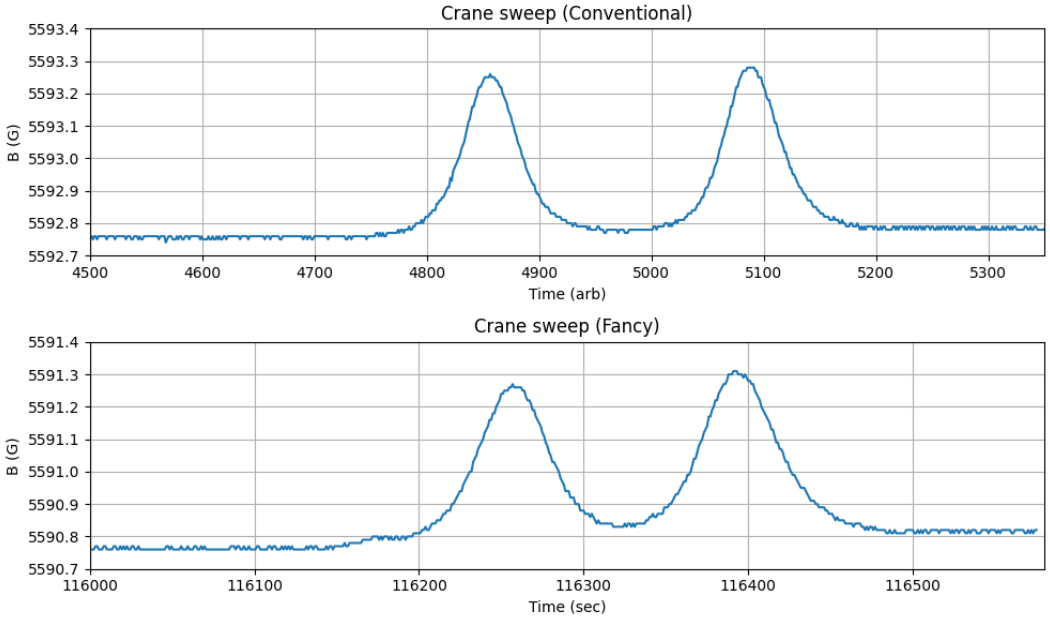

Figure 7: Effect of crane-sweep on the magnetic field for both conventional (top) and fancy ramp-up (bottom). The bump amplitude caused by the sweep are similar at about 0.5 G for both sweeps. The average field difference before and after the crane-sweep is about 25 mG and 54 mG for conventional and fancy ramp-up respectively. (Note that the results from conventional ramp-up was obtained a year before the test for fancy-ramp up.)

5.3 Field Droop

To get a sense of the long-term stability of the magnetic field, the NMR probe data was collected over night after the fancy ramp-up. The result is shown in Fig. 8.

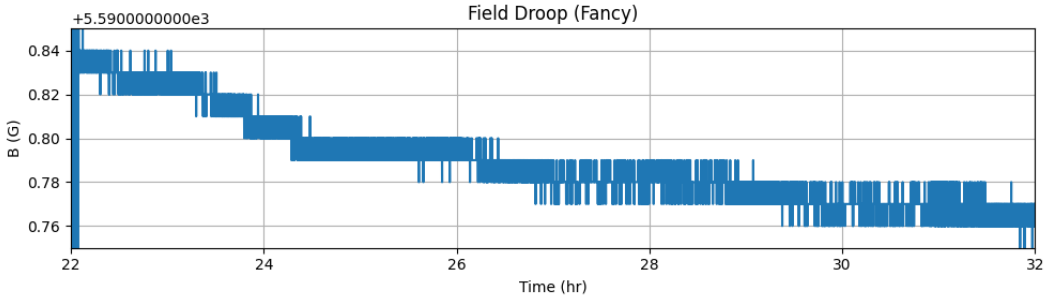

Figure 8: The overnight magnetic field observed by the NMR probe after the fancy ramp-up. The field droop in 10 hours is about 80 mG, i.e. 0.0014% of the average field.

6 Simulation study

A 2D axially symmetric model is constructed to simulate the propagation of magnetization within the main magnet yoke and pole during ramp-up. The purpose of the simulation model is to try to determine the sources of the time-dependant behaviours exhibited by the magnet.

While the simulation model is only 2D, comparing the simulations with and without eddy-currents show that eddy-currents are largely responsible for the radial-dependence of the field ramping rate. The simulation reproduce the "overshoot" effect observed in the real magnet at higher radii.

It is also worth noting that the valleys between the magnet sectors have no magnetic yoke to capture the magnetic flux. This is may partially explain some of the disagreements between the measurements and the 2D model, as there may be some time-dependant azimuthal variation in the magnetization within the pole as well.

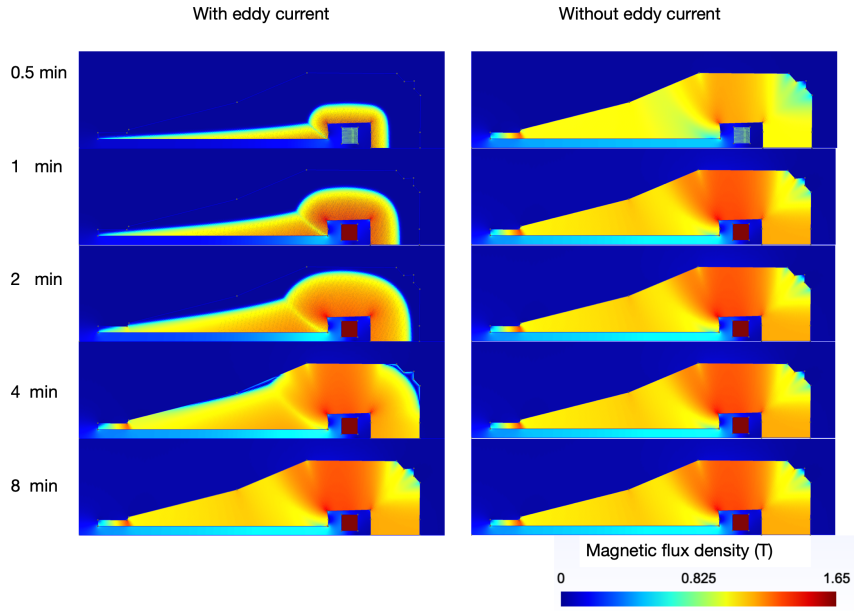

Figure 9: Propagation of magnetization with and without consideration of eddy currents. In both models, the magnet is linearly ramped up from 0 to 18130 A over a period of 1 minutes. The left column displays the field distribution without considering eddy currents. Initially, the iron is uniformly magnetized, followed by saturation of the upper yoke, the vertical yoke, and the pole region. When the current in the coil reaches the maximum, the inner radius of the pole becomes more saturated than the outer radius. The right column displays the field distribution while considering eddy currents. The skin effect caused by eddy currents initially concentrates the magnetic field on the inner surface of the magnet, closer to the coil. This concentrated magnetic field drives the saturation of the iron on the inner surface first, and the magnetic field gradually propagates to the whole magnet. The final distribution of magnetization in the iron is identical in both models.

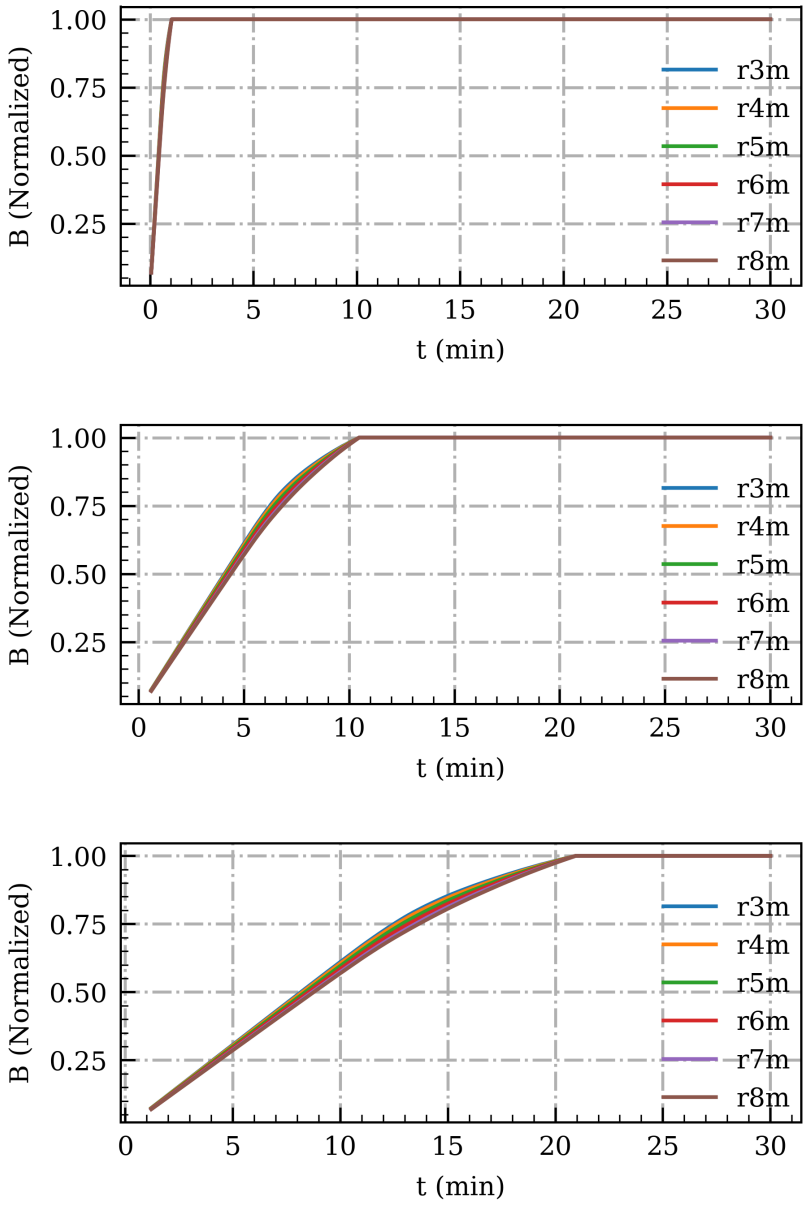

Figure 10: The normalized axial magnetic field B_z at various radii on the median plane of the magnetostatic model. The field is normalized by the final static field at each point. For different ramp-up speeds, when the coil current reaches its maximum value, the field at different positions also reaches its maximum value, indicating no delay between the coil current and magnetic field. However, the ramp-up curves of the field at different radii do not overlap, with the outer radius ramping up more linearly. This observation is consistent with the results shown in Figure 9, where the magnetization of the iron in the pole region is more saturated at the inner radius than the outer radius. The magnetostatic model can't explain the experiment data, in which the field at outer radius ramps up more rapidly initially and then slows down when the coil current becomes large.

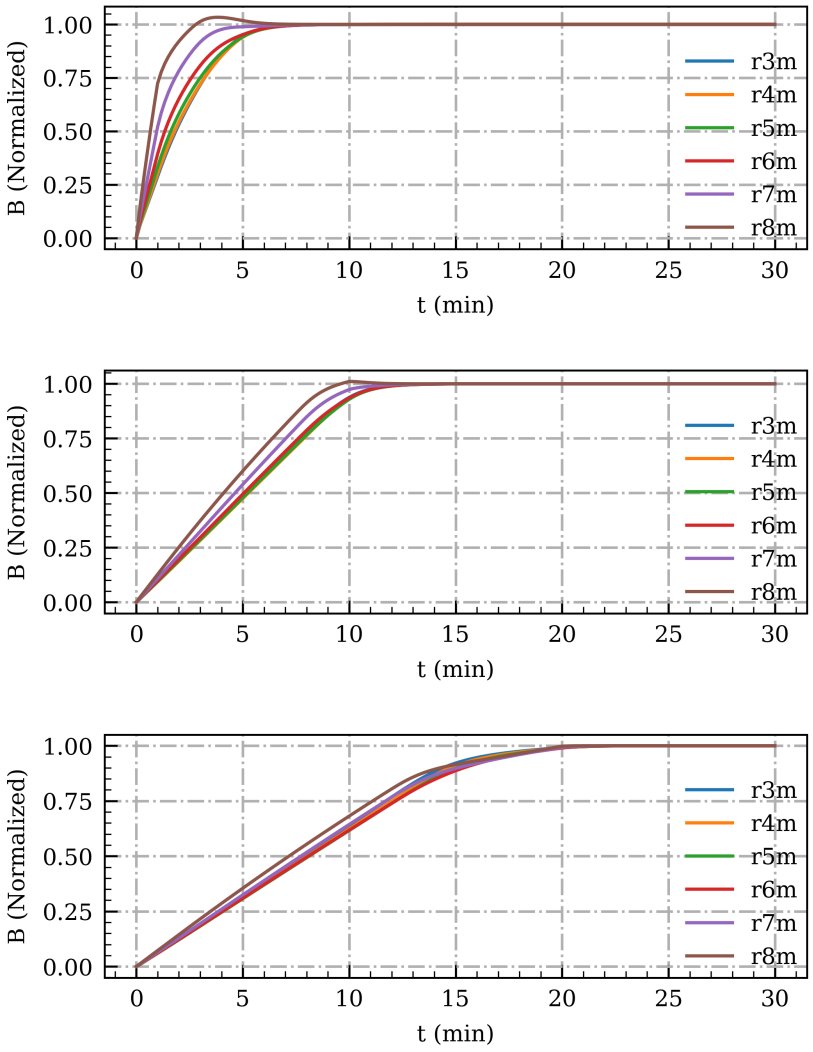

Figure 11: The normalized axial magnetic field B_z at various radii on the median plane of the diffusion model which takes into account the eddy current in the magnet. The skin effect in the diffusion model causes the field to propagate from the surface close to the coil to further locations in the magnet. As a result, the field at the outer radius ramps up more quickly at the beginning, saturating the iron and then slowing down. This behaviour can explain the double crossover observed in the experimental data. The relaxation time for the propagation of the magnetization is estimated to be several minutes, as shown by (a) and (b). However, the delay caused by the eddy current in the simulation model is much greater than that observed in the experimental data. A possible explanation for this discrepancy is that the magnet is constructed from laminated iron pieces, which reduces the eddy current.

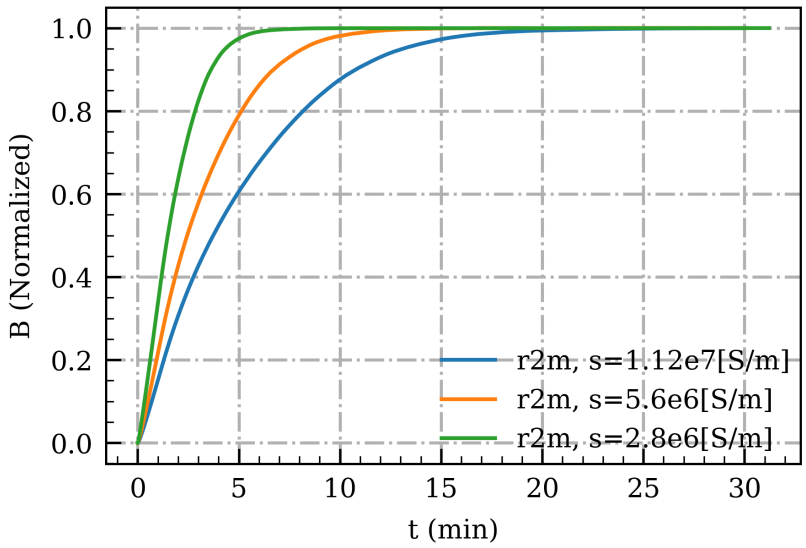

Figure 12: We simulated the magnetic field at a radius of 2 meters under different electrical conductivities of the magnet while ramping up the magnet linearly to 18130 A over a period of 1 minute. The blue line represents the model using the electrical conductivity of solid iron. The relaxation time of this model is approximately 20 minutes. By arbitrarily reducing the electrical conductivity to mimic the laminated structure of the magnet, the impact of eddy currents can be reduced, resulting in a decrease in the delay of the field propagation.

7 Procedure

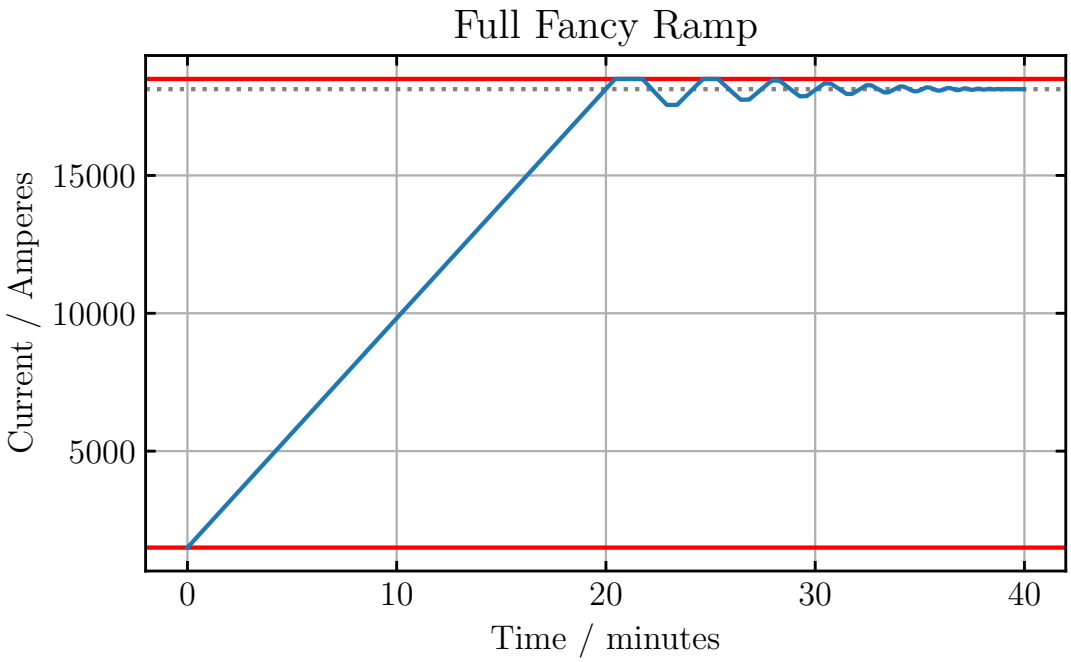

Figure 13: The full fancy rampup procedure is plotted. The operational current limits of the power supply are shown as red horizontal lines. The final setpoint of 18.125 kA is shown as a grey dotted line, to guide the eye.

The final procedure decided on is the 20 min+20 min fancy ramp shown in Fig. 13. That is, a 20 min ramp to the final setpoint followed by an oscillation period of another 20 min, about the final setpoint. The oscillation part of the procedure is shown in greater detail in Fig. 14. This ramp rate balances the total time the procedure takes with the final accuracy and reproducibility of the field. The details of the fancy ramp, and the HLA running it, will be published in a document to come.

The field stability testing showed that the fancy ramp was much more robust over time and also when exposed to large perturbations. We hope that the stability demonstrated will reduce tuning times and aide in machine recovery after unexpected delivery interruption.

The software used to record the field measurements needs much more refinement if it were to be used again in the future. The LakeShore Gaussmeter is well documented and easy to work with, however, the length of the probe cables limited the maximum radial span we could measure, and hence limited our capability to measure the field non-uniformity.

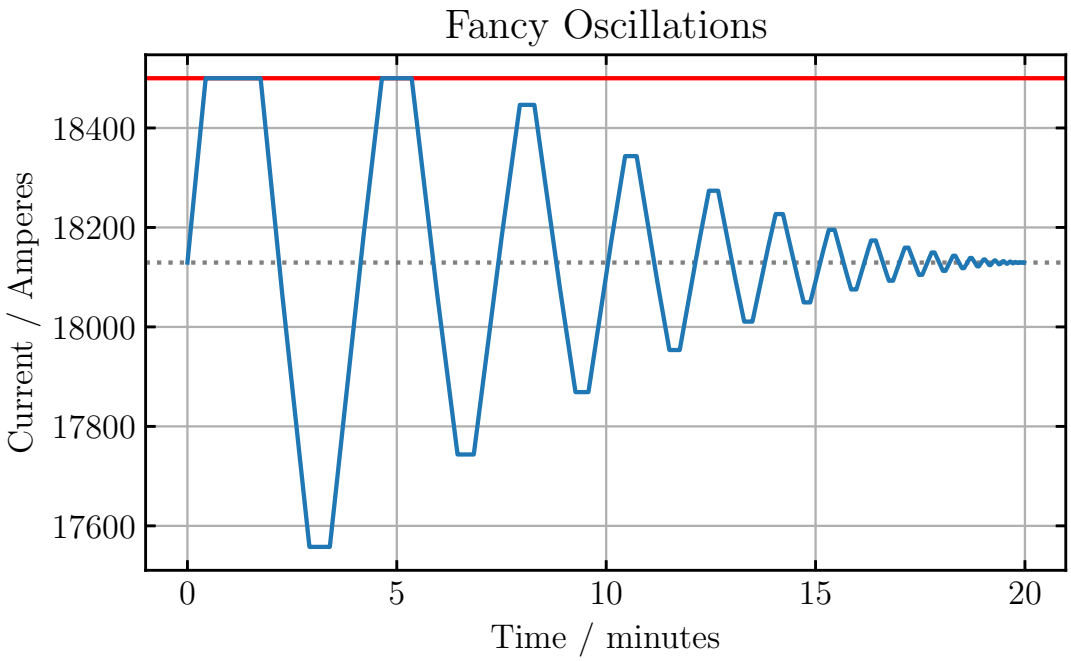

Figure 14: The last 20 min of the fancy rampup procedure, just the oscillations, are shown. The operational current limit of the power supply is shown as a red horizontal line. The final current setpoint of 18.125 kA is shown as a grey dotted line, to guide the eye. Note the two following features: the amplitude of the oscillations would exceed the max current but is instead cut-off and that the procedure waits at the extrema of each oscillation.

References

[1] S. Carrozza, et al., The New 20 kA 80 V Power Supply for the 520 MeV H- Cyclotron at TRIUMF, in: Proc. 9th International Particle Accelerator Conference (IPAC'18), Vancouver, BC, Canada, April 29-May 4, 2018, no. 9 in International Particle Accelerator Conference, JACoW Publishing, Geneva, Switzerland, 2018, pp. 3792–3795, https://doi.org/10.18429/JACoW-IPAC2018-THPAL062. doi:doi:10.18429/JACoW-IPAC2018-THPAL062.
URL http://jacow.org/ipac2018/papers/thpal062.pdf

[2] S. Carrozza, et al., A New Concept of High Current Power Supply for the Main Cyclotron Magnet at TRIUMF, in: Proc. of International Conference on Cyclotrons and Their Applications (Cyclotrons'16), Zurich, Switzerland, September 11-16, 2016, no. 21 in International Conference on Cyclotrons and Their Applications, JACoW, Geneva, Switzerland, 2017, pp. 186–189, doi:10.18429/JACoW-Cyclotrons2016-TUP10. doi:doi:10.18429/JACoW-Cyclotrons2016-TUP10.
URL http://jacow.org/cyclotrons2016/papers/tup10.pdf

[3] J. Nasser, R. Baartman, O. Kester, S. Kiy, T. Planche, S. Rädel, O. Shelbaya, Algorithm to Mitigate Magnetic Hysteresis in Magnets with Unipolar Power Supplies, in: Proc. IPAC'22, no. 13 in International Particle Accelerator Conference, JACoW Publishing, Geneva, Switzerland, 2022, pp. 156–159. doi:10.18429/JACoW-IPAC2022-MOPOST039.
URL https://jacow.org/ipac2022/papers/mopost039.pdf

[4] K. Reiniger, H. Baumann, D. Dohan, D. Pearce, Stability improvements in the TRIUMF cyclotron magnetic field to ±0.7 ppm, Le Journal de Physique Colloques 45 (C1) (1984) C1–225.

[5] J. Burgerjon, O. Fredriksson, A. Otter, W. Grundman, B. Stonehill, Construction details of the TRIUMF H^- cyclotron, IEEE Transactions on Nuclear Science 20 (3) (1973) 243–247.